Supplementary information

Enabling 3D Printability and Vascular Morphogenesis with Double Network Dynamic Hydrogels

Runze Xu [a], Bohan Dou [a], Shuang Yu [a], Ziyu Wang [c], Yanli Zhang [e], Ling Leng [d], Liliang Ouyang [a, b,], Wei Sun [a]*

[a] Biomanufacturing and Rapid Forming Technology Key Laboratory of Beijing, Biomanufacturing and Engineering Living Systems Innovation International Talents Base (111Base), Department of Mechanical Engineering, Tsinghua University, Beijing 100084, China

[b] State Key Laboratory of Tribology in Advanced Equipment, Tsinghua University, Beijing, 100084, China

[c] Department of Orthopedics, Peking University Third Hospital, Beijing, 100191, China.

[d] Stem cell and Regenerative Medicine Lab, Department of Medical Science Research Center, State Key Laboratory for Complex, Severe, and Rare Diseases, Center for Translational Medicine, Peking Union Medical College Hospital, Chinese Academy of Medical Sciences and Peking Union Medical College, Beijing 100730, China.

[e] Imaging Core Facility, Technology Center for Protein Science, Tsinghua University, Beijing 100084, China

* Corresponding author.
E-mail address: Ouyang, L. (ouy@tsinghua.edu.cn)

Figure S1-S19

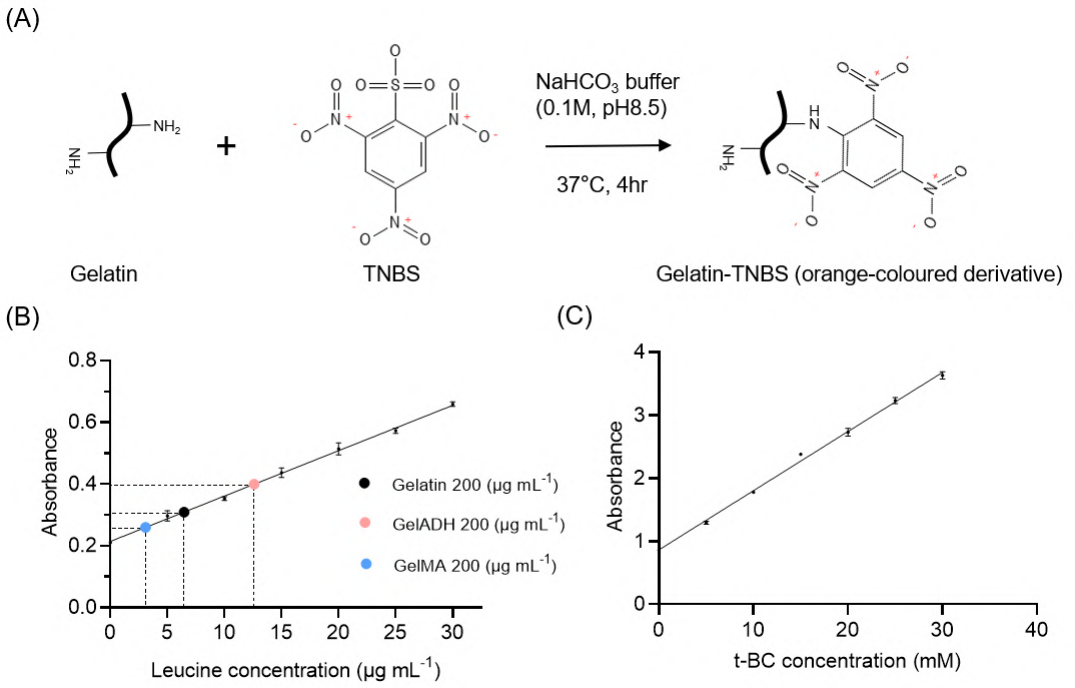

Figure S1. Quantification of modification degree of the hydrogel components in the DNDH system. (A) Schematic illustration of the TNBS assay used to quantify the primary amines of Gelatin, GelMA and GelADH. (B) Leucine concentration range from 0-30 μg mL^{-1} are used to generate a standard curve to determine the amounts of primary amines that are replaced by modified functional groups. (C) The DexCHO modification was also quantified by the TNBS assay, where t-BC was reacted with the DexCHO, and the reacted products were further quantified with TNBS.

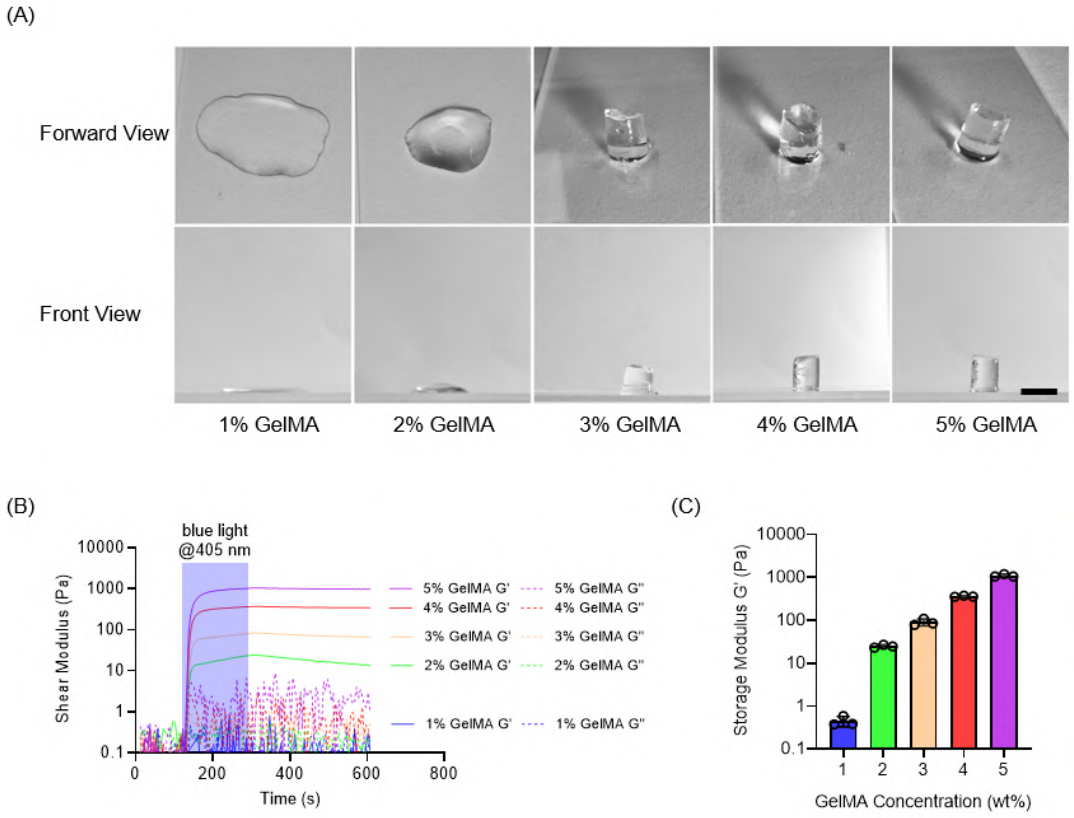

Figure S2. Screening a suitable concentration of GelMA that serves as a stable base hydrogel component to formulate the DNDH. (A) Shape fidelity of GelMA with different concentrations from 1 wt%-5 wt%. (B) Rheological time-sweep of GelMA hydrogel in the presence of blue light indicates the gelation process of GelMA under different concentrations, under the light exposure of 30 mW cm^{-2} for 3 min. (C) Quantification of the storage modulus of GelMA hydrogels at pleatue stage (N=3). Scale bar: 500 μm (A).

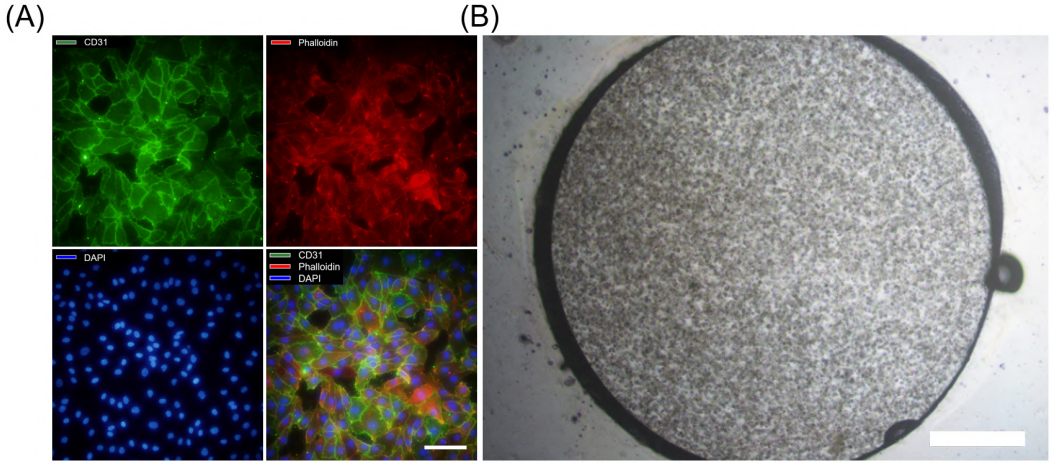

Figure S3. Verification of the HUVECs, and the hydrogel embedding process. (A) The HUVECs cells used in this study consistently express CD31, labelled in green. The red and blue represent phalloidin and DAPI, respectively. (B) A representative photo of the hydrogels that

embed the HUVECs within the customized disc mould at Day 0. Scale bars, 100 μm (A) and 1000 μm (B).

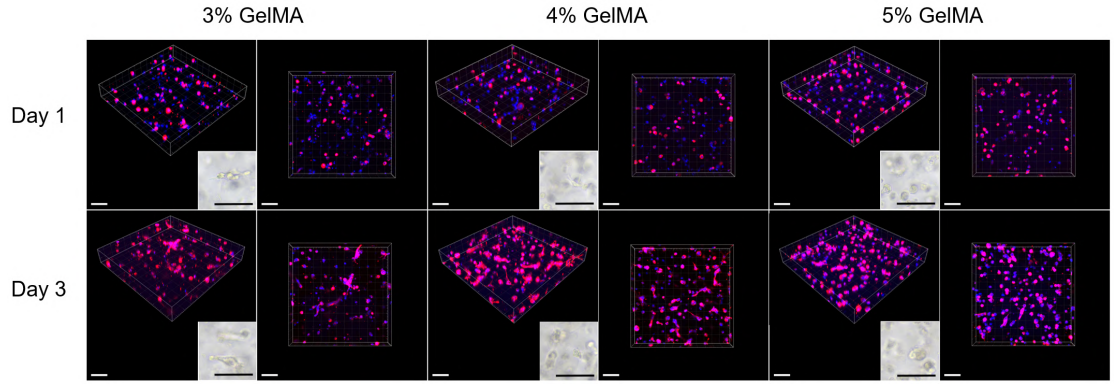

Figure S4. Screening the suitable GelMA concentration for the 3D culture of HUVECs. The HUVECs were cultured in 3 wt%-5 wt% GelMA hydrogel and cultured for 3 days. The cell morphology was observed with the cellular skeleton labelled by phalloidin in red, and the cell nucleus labelled by DAPI in blue. Scale bar, 100 μm.

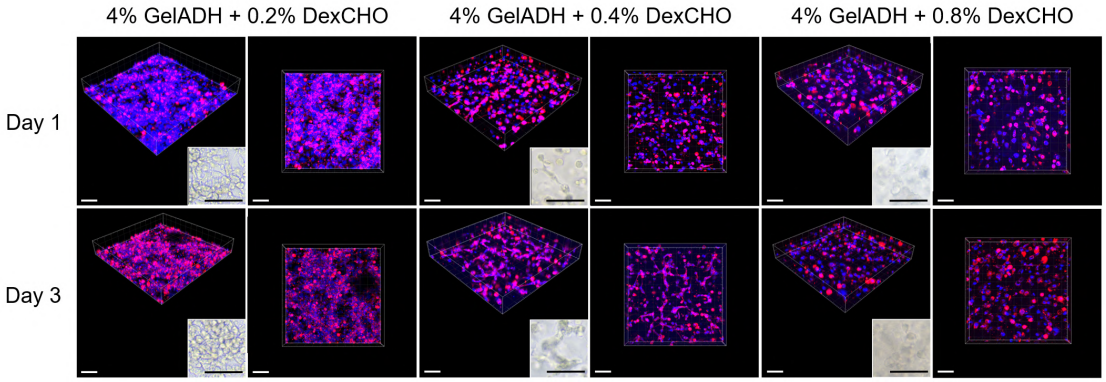

Figure S5. Screening the suitable DexCHO crosslinker concentration for the 3D culture of HUVECs in dynamic hydrogels based on a fixed GelADH concentration at 4 wt%. After 3D culturing in the GelADH hydrogel for 3 days, the cell morphology was observed with the cellular skeleton labelled by phalloidin in red, and the cell nucleus labelled by DAPI in blue. Scale bar, 100 μm.

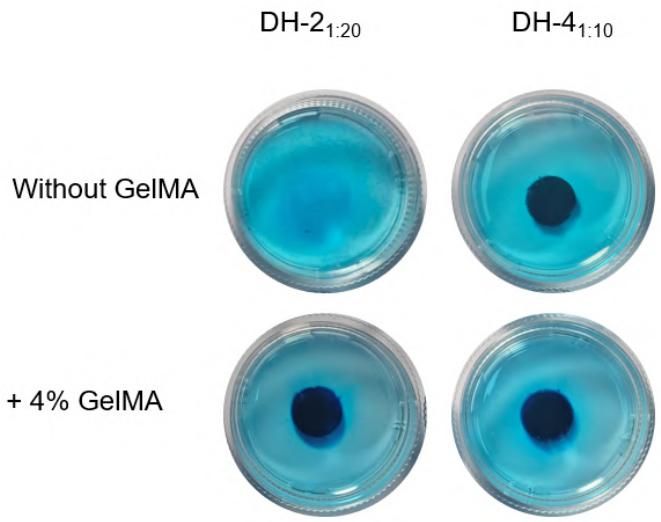

Figure S6. Representative photos of pre-fabricated hydrogel discs in phosphate buffer saline (PBS) show the structural stability in hydrated conditions. The DHs are stabilized with the addition of 4 wt% GelMA and photo-crosslinking, while the relatively weak DH group is degraded without introducing the GelMA component.

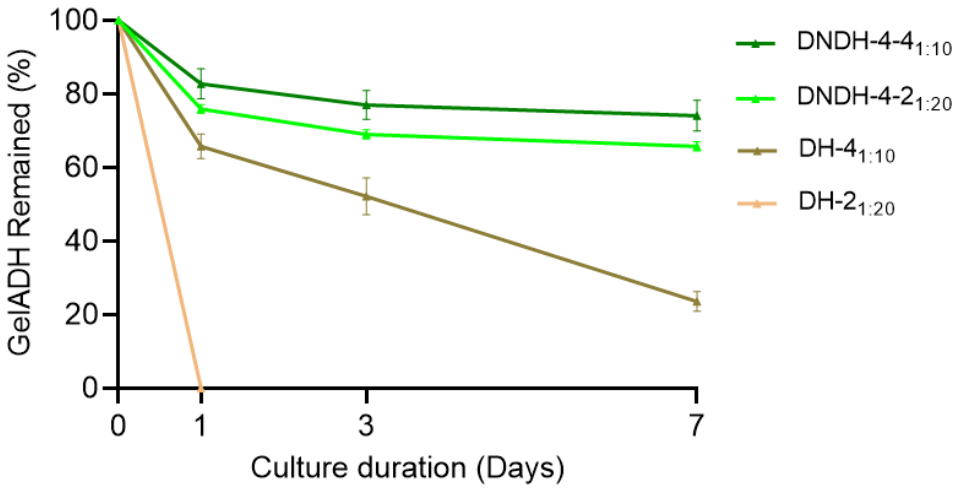

Figure S7. Assessing the retention of dynamic hydrogel component in the DHs and the DNDHs over incubation in PBS at 37°C for 7 days.

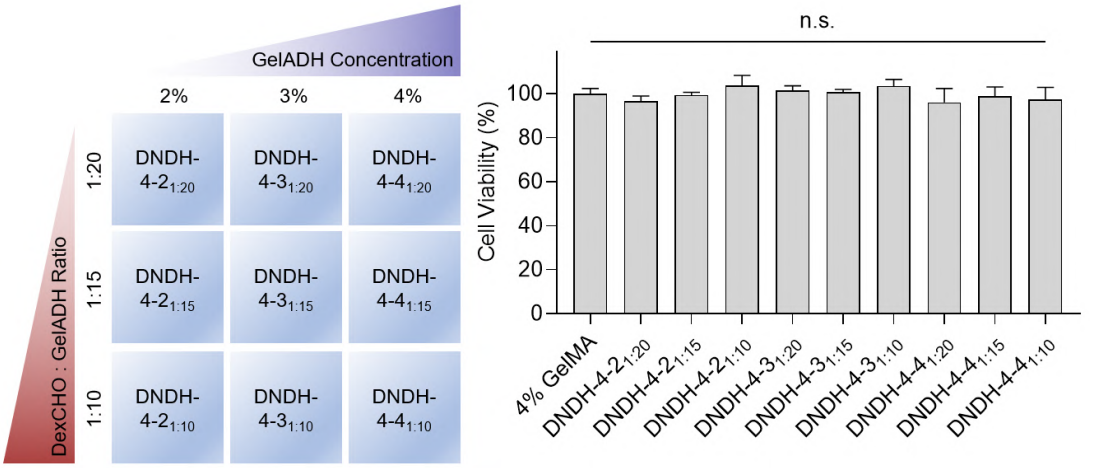

Figure S8. Cell viability test (CCK8 assay) of the HUVECs embedding into the DNDHs after incubation at 37°C and 5 % CO_2 for 24 h. The 4 wt% GelMA group served as a control group and the cell viability of the DNDH groups was normalized to the 4 wt% GelMA group. Statistical significance was indicated by: n.s. $p > 0.05$. N=3

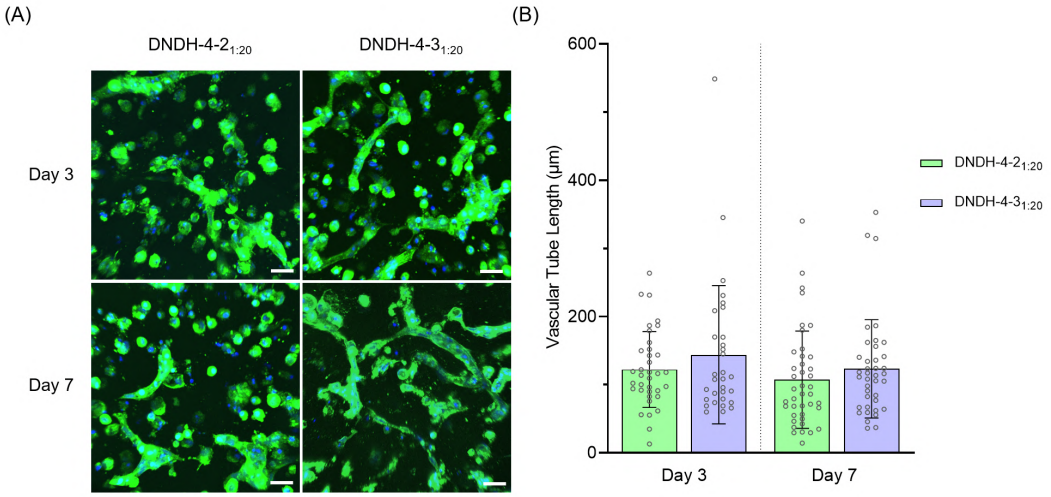

Figure S9. (A) Zoomed-in view of the HUVECs cultured in the DNDH-4-$2_{1:20}$ and DNDH-4-$3_{1:20}$ groups. The cells were stained with CD31 in green, and the cell nucleus labeled with DAPI in blue. (B) Quantification of vascular tube length in the DNDH-4-$2_{1:20}$ and DNDH-4-$3_{1:20}$ groups. Scale bars, 30 μm.

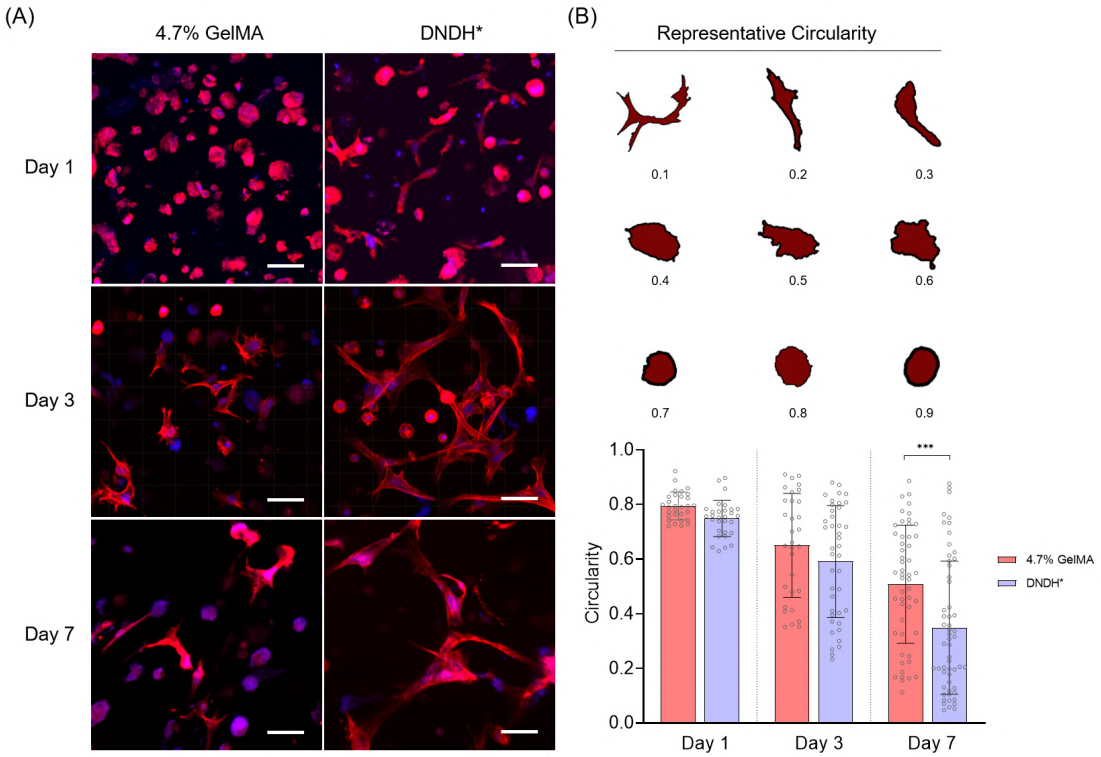

Figure S10. (A) Representative images of hMSC cells embedded in the 4.7% GelMA and DNDH*. The cell morphology was observed with the cellular skeleton labelled by phalloidin in red, and the cell nucleus labelled by DAPI in blue. (B) Quantification of the aspect ratio of hMSC cells. Scale bars, 50 μm. Statistical significance was indicated by: ***$p \leq 0.001$.

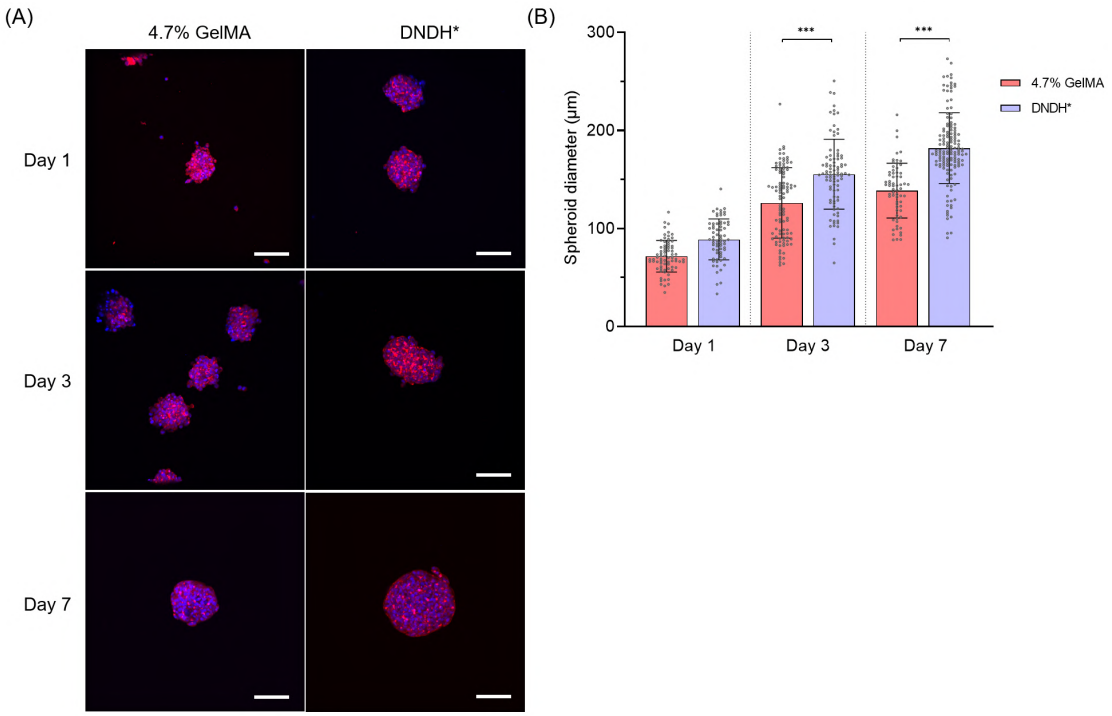

Figure S11. (A) Representative images of HepG2 spheroids cultured in the 4.7% GelMA and DNDH*. The cell morphology was observed with the cellular skeleton labelled by phalloidin

in red, and the cell nucleus labeled by DAPI in blue. (B) Quantification of the size of HepG2 spheroids. Scale bars, 100 μm. Statistical significance was indicated by: ***p ≤ 0.001.

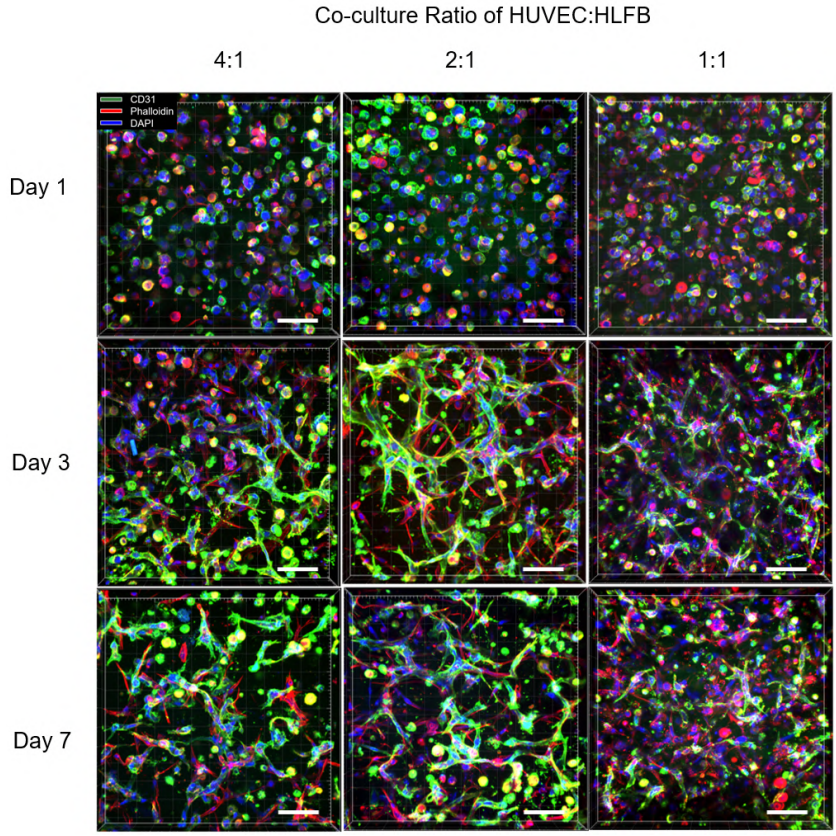

Figure S12. Optimization of vascular network formation in the DNDH* group by adjusting the HUVECs:HLFB ratio. The HUVECs:HLFBs ratio was controlled from 4:1 to 1:1 with a fixed cell density of HUVECs at 4 million cells mL^{-1}, co-cultured for 7 days. The cells were stained for CD31 in green, the cell skeleton labeled with phalloidin in red, and the cell nucleus labeled with DAPI in blue. Scale bars, 100 μm.

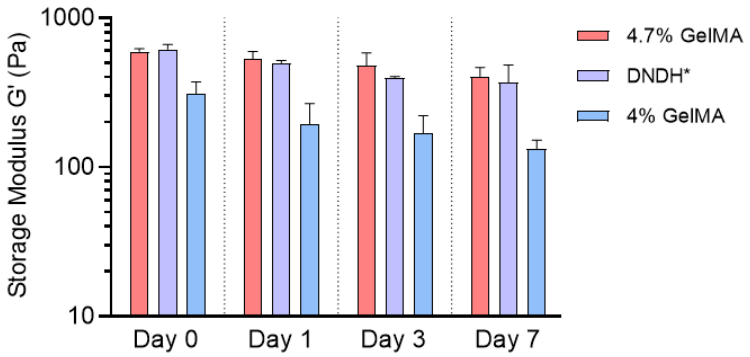

Figure S13. Quantifying the hydrogel stiffness over a 7-day culturing period in the presence of HUVECs and HLFB (2:1 ratio).

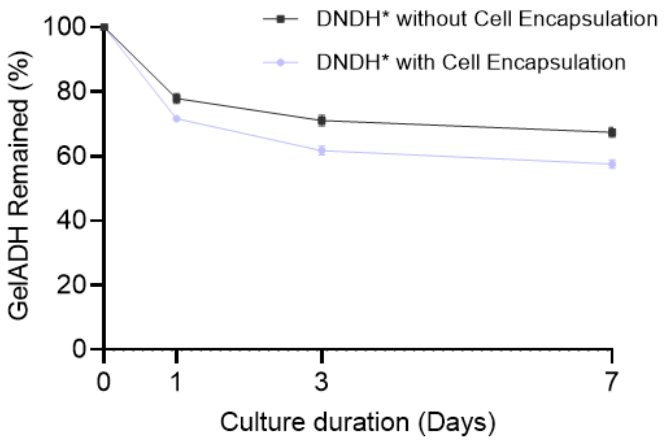

Figure S14. Determining the remaining content of GelADH in the DNDH* group for 7 days, with or without HUVECs and HLFBs co-embedding.

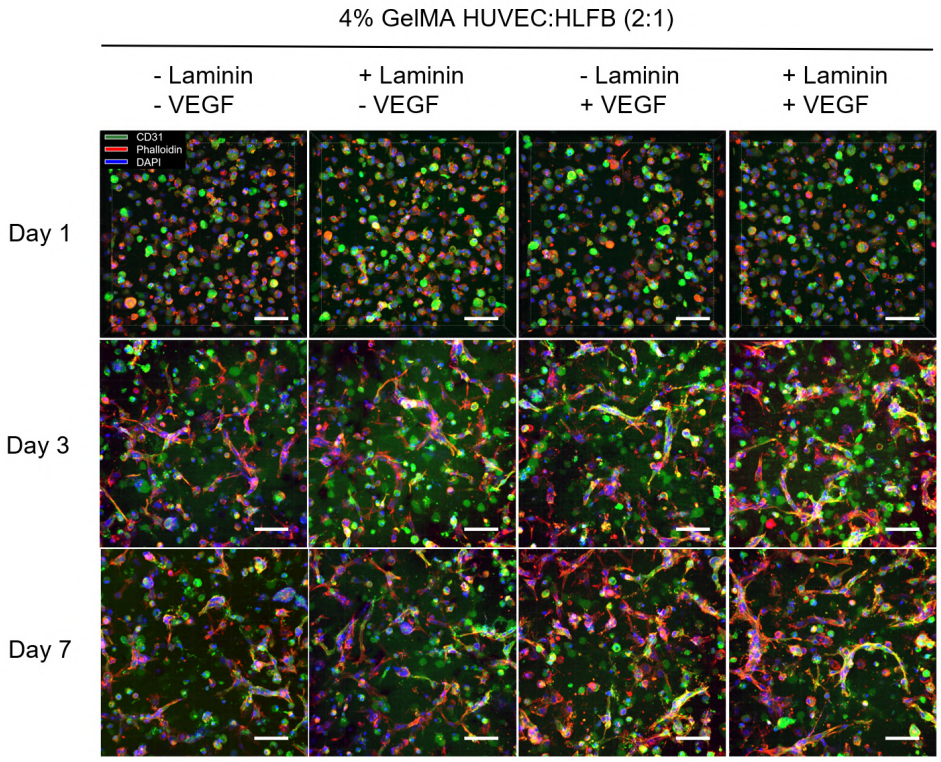

Figure S15. Visualization of the co-cultured vascular network formation in the 4 wt% GelMA group in the presence or absence of laminin and VEGF. The cells were stained for CD31 in green, the cell skeleton labeled with phalloidin in red, and the cell nucleus labeled with DAPI

in blue. It was determined that the simultaneous addition of laminin and VEGF improved the vascular network formation by assessing the vascular tube length and mean tube volume. Scale bars, 100 μm.

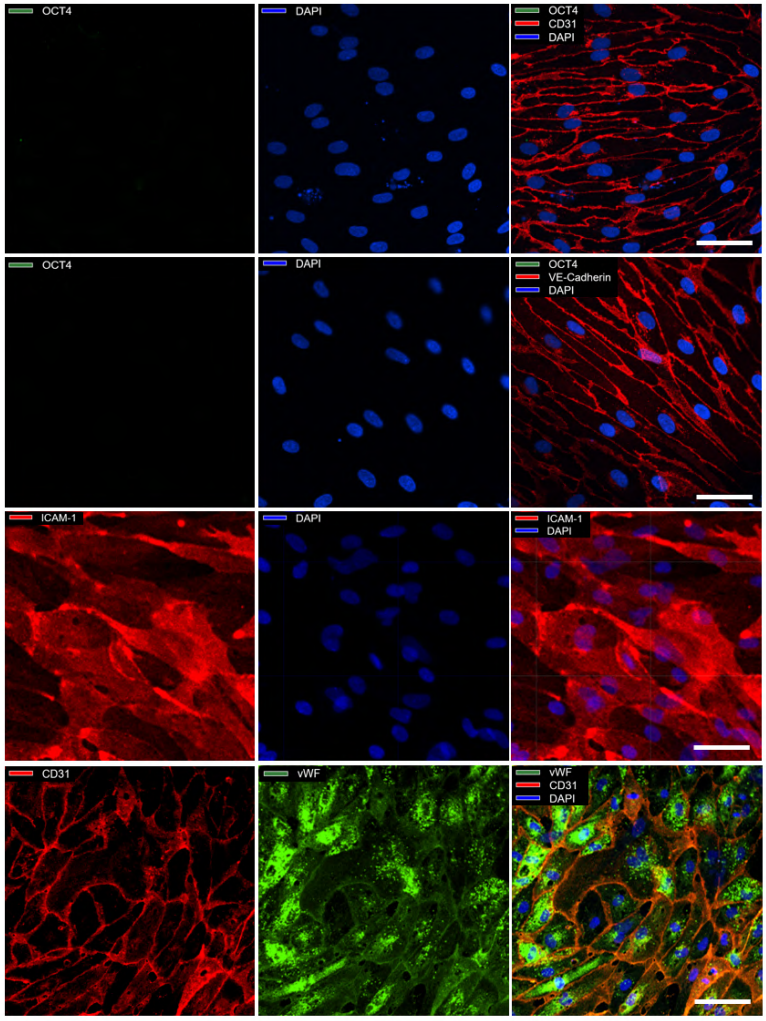

Figure S16. Characterization of typical markers expressed by the iPSCs-derived ECs. Scale bars, 50 μm.

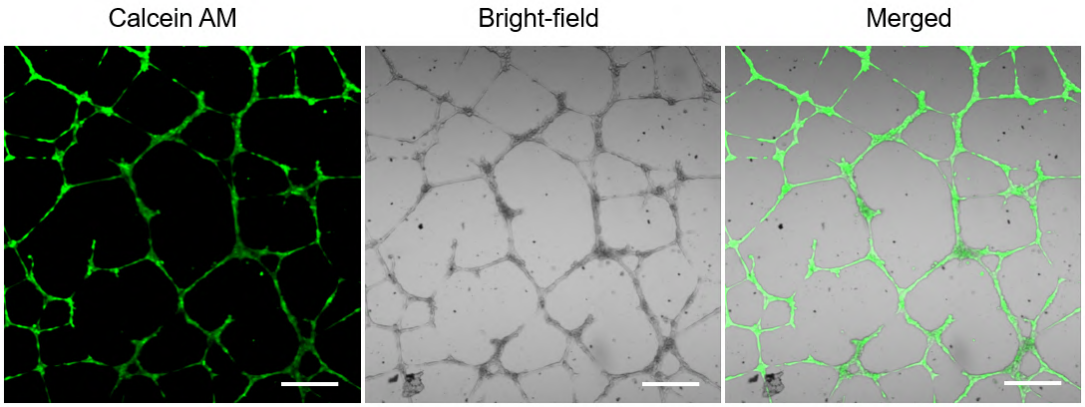

Figure S17. Verifying the vascular reorganization function of iPSCs-derived ECs using the *in vitro* Matrigel tubing assay. Scale bars, 500 μm.

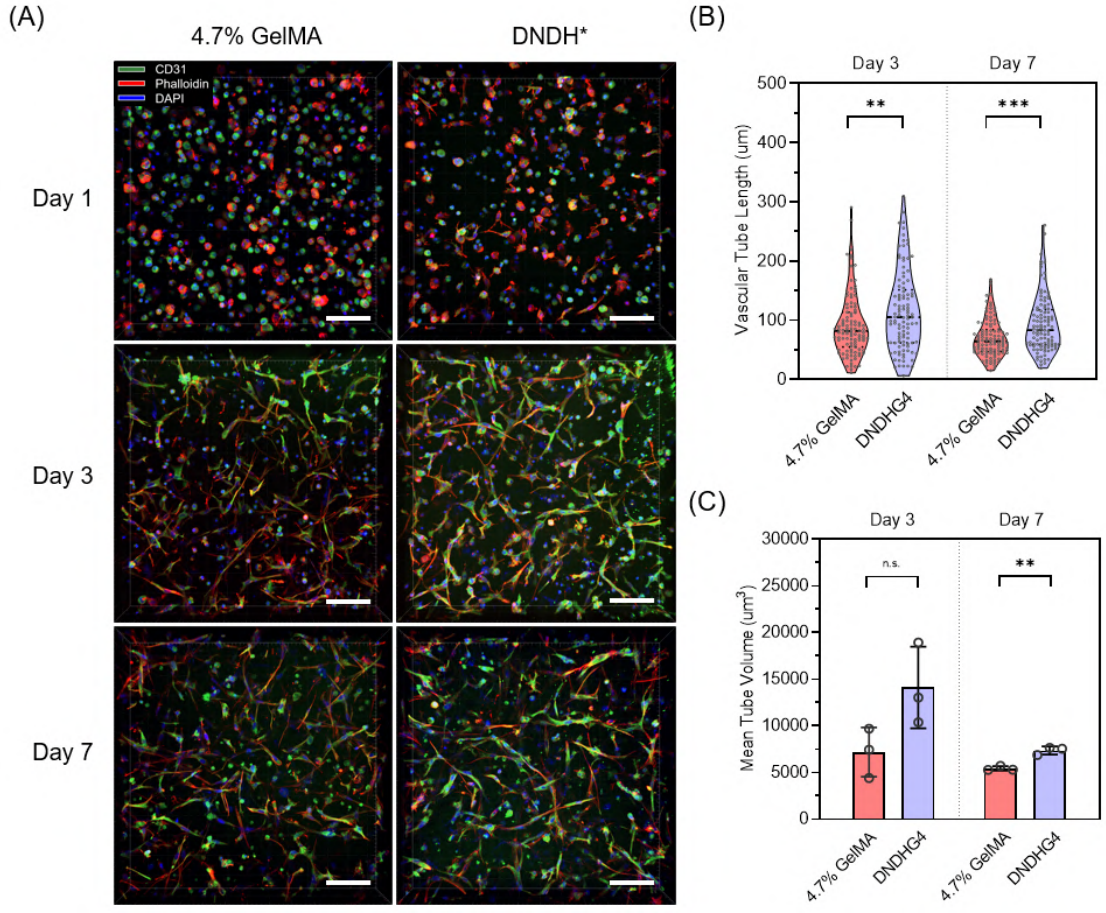

Figure S18. Vascular formation of iPSC-derived ECs confirms the benefit of matrix dynamics in DNDH. (A) Representative confocal images of co-cultured iPSC-derived ECs and HLFBs embedded in the 4.7 wt% GelMA and DNDH* groups, both with the addition of extra biochemical cues of laminin and VEGF. The cells were stained for CD31 in green, cell skeleton labelled with phalloidin in red, and cell nucleus labelled with DAPI in blue. (B), (C): It was concluded that, when using the iPSC-derived ECs, the DNDH* still supports greater vascular networks formation compared to that in the GelMA group at similar stiffness. Scale bars, 100 μm. Statistical significance was indicated by: n.s. $p > 0.05$, **$p \leq 0.01$, and ***$p \leq 0.001$.

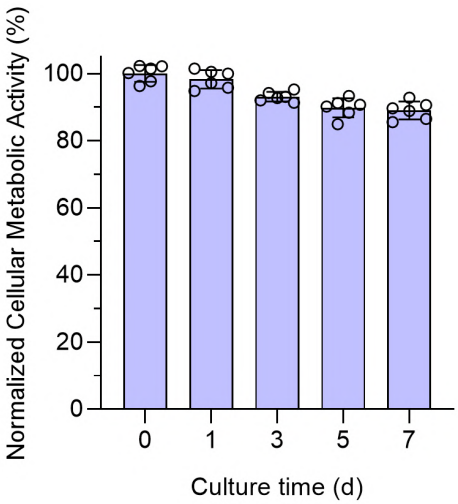

Figure S19. Assessing the general cellular metabolic activity of the HUVECs and HLFBs in the printed DNDH* constructs over a culture period of 7 days, using the alamarBlue™ assay.

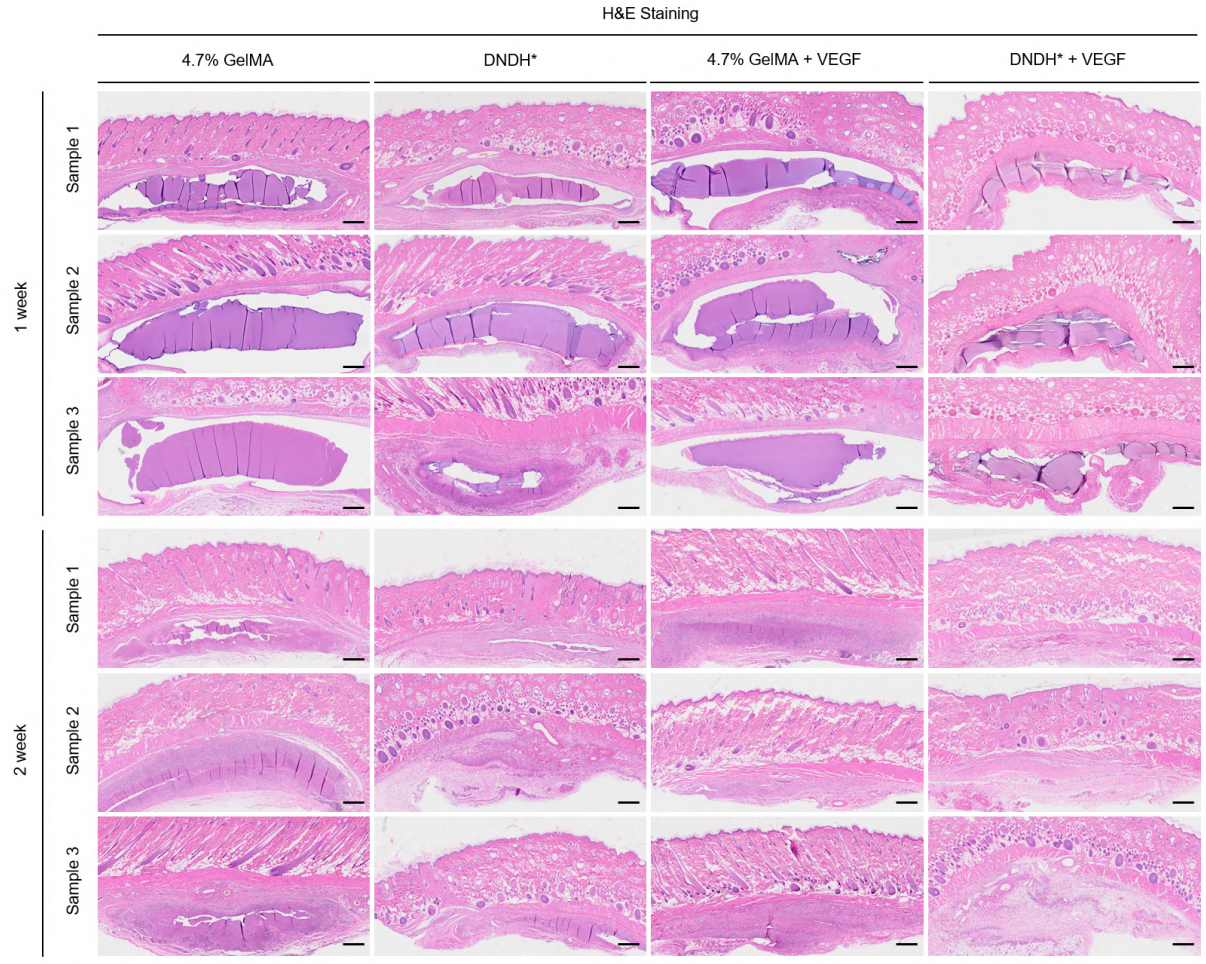

Figure S20. H&E staining of the hydrogel sections to assess cell ingrowth from peripheral tissue. The subcutaneous region that contains the hydrogel is shown (n = 3), Scale bars, 500 μm.

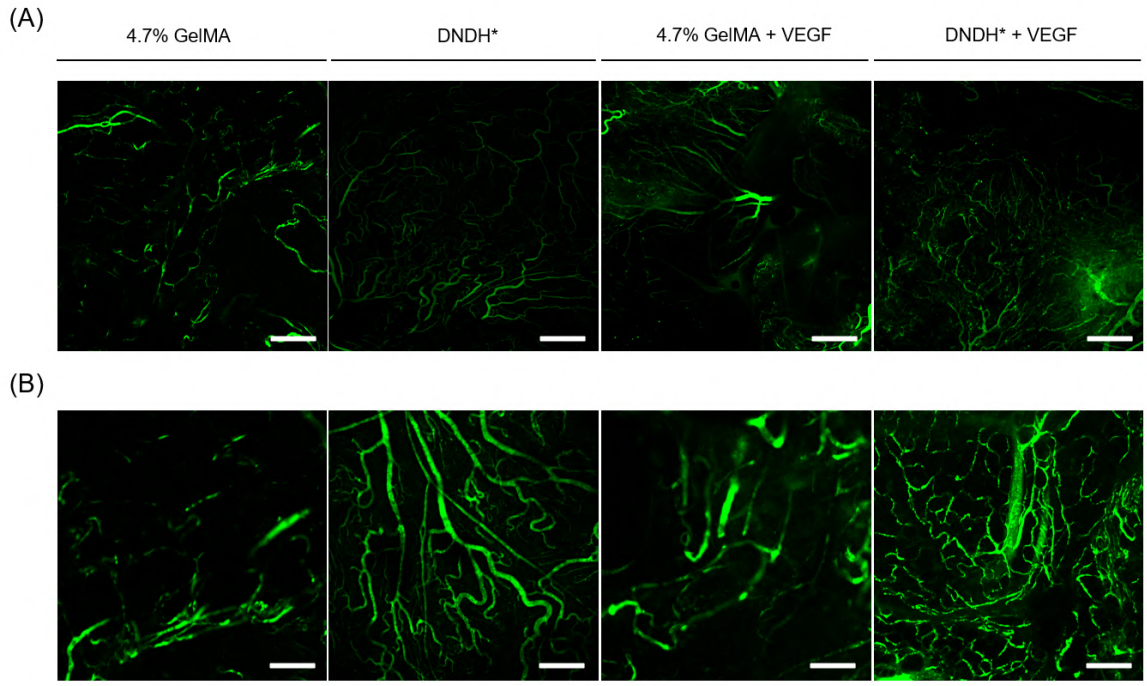

Figure S21. (A) Visualizing the established blood vessels in the subcutaneous transplanted hydrogels at 2 weeks. Before harvesting and visualizing the transplanted hydrogels, the SD rats were injected with Dextran-FITC through the tail vein. (B) Visualization at higher magnification. Scale bars, 500 μm (A), 200 μm (B).

Graphical Abstract

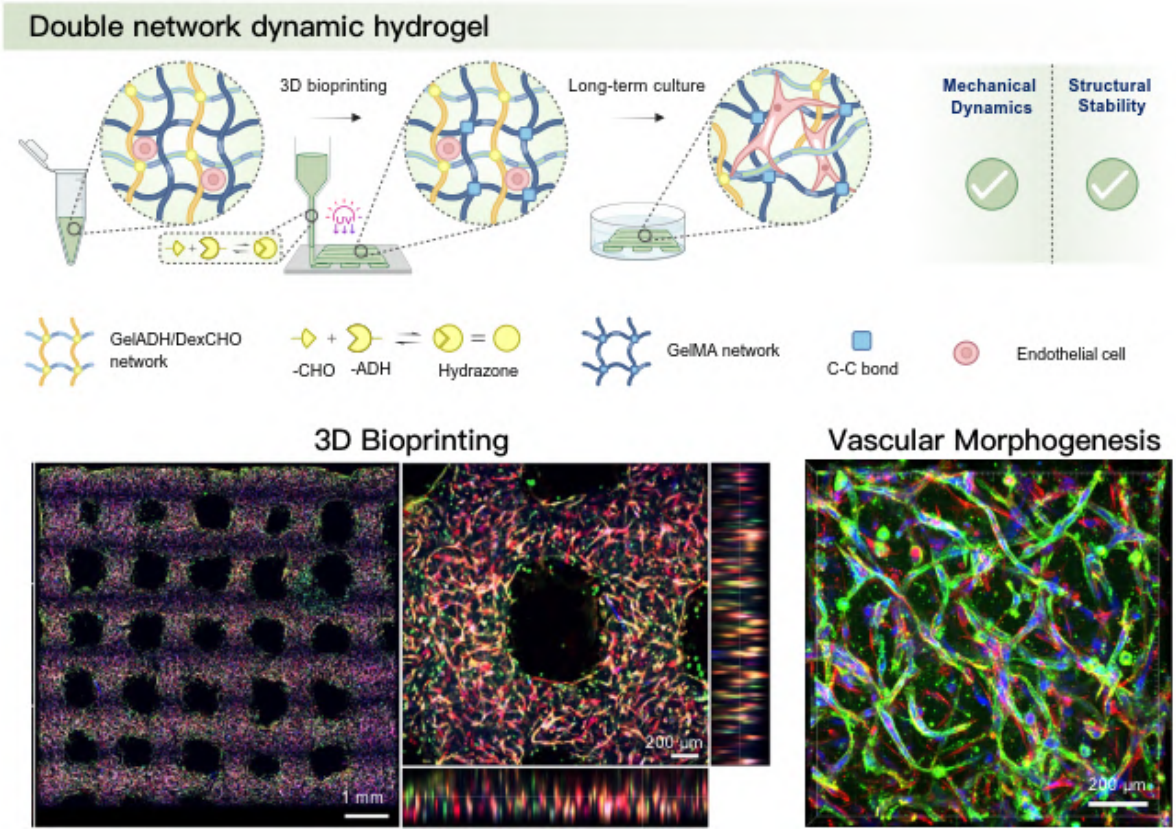

Declaration of interests

☐ The authors declare that they have no known competing financial interests or personal relationships that could have appeared to influence the work reported in this paper.

☒ The author is an Editorial Board Member/Editor-in-Chief/Associate Editor/Guest Editor for *Biomaterials Advances* and was not involved in the editorial review or the decision to publish this article.

☒ The authors declare the following financial interests/personal relationships which may be considered as potential competing interests:

W. Sun, L. Ouyang and R. Xu has applied for a Chinese Patent related to this study (file No. 2023080479). Other authors declare no conflict of interest.